



The composite development and structure of intense synoptic-scale Arctic cyclones

Alexander F. Vessey¹, Kevin I. Hodges^{1,2}, Len C. Shaffrey^{1,2}, and Jonathan J. Day³

¹Department of Meteorology, University of Reading, Earley Gate, Reading RG6 6BB, UK

²National Centre for Atmospheric Science, University of Reading, Earley Gate, Reading RG6 6BB, UK

³ECMWF, Shinfield Park, Reading RG2 9AX, UK

Correspondence: Alexander F. Vessey (alecvessey@hotmail.co.uk)

Abstract.

Understanding the location and intensity of hazardous weather across the Arctic is important for assessing risks to infrastructure, shipping, and coastal communities. A key driver of these risks are the high winds, high ocean waves and heavy precipitation, which are dependent on the structure and development of intense synoptic-scale cyclones. This study aims to describe the typical lifetime, structure, and development of a large sample of past intense winter (DJF) and summer (JJA) synoptic-scale Arctic cyclones, using a storm compositing methodology applied to the ERA5 reanalysis. Results show that the composite development and structure of intense Arctic summer cyclones is different to that of intense winter Arctic and North Atlantic Ocean extra-tropical cyclones, and to that described in conceptual models of extra-tropical and Arctic cyclones. The composite structure of intense Arctic summer cyclones shows that they typically undergo a structural transition around the time of maximum intensity from having a baroclinic structure to an axi-symmetric cold-core structure throughout the troposphere, with a low-lying tropopause and large positive temperature anomaly in the lower stratosphere. Arctic summer cyclones are also found to have longer lifetimes than these other cyclones, potentially causing prolonged hazardous and disruptive weather conditions in the Arctic.

1 Introduction

Recent reductions in Arctic sea ice extent (Stroeve et al., 2012; National Snow & Ice Data Centre, 2020) have opened up shorter shipping routes between ports in North America, Europe, and Asia (Melia et al., 2016), access to previously inaccessible natural resources such as oil (Harsem et al., 2015), and new destinations for tourism (Maher, 2017). Consequently, the number of ships navigating the Arctic with people and valuable goods has increased in recent years (Babin et al., 2020; Li et al., 2021). Given that Arctic sea ice extent will continue to reduce over the 21st century in response to further global warming (Stroeve et al., 2007, 2012), human activity in the Arctic is expected to increase further as the Arctic becomes increasingly navigable. But as the Arctic becomes increasingly used for shipping, oil exploration and tourism, the exposure to hazardous weather associated with Arctic cyclones, may increase.

The structure of extra-tropical cyclones has been a focal point of scientific research for over 100 years, as they can have a damaging impact on populous areas such as Europe (Browning, 2004; Leckebusch et al., 2007; Pinto et al., 2012). Bjerknes



25 (1919, 1922) were among the first to describe the typical structure and locality of hazardous weather within extra-tropical
cyclones, and proposed the Norwegian Cyclone Model - a conceptual model of extra-tropical cyclone development and
structure. It is now understood that the locality of hazardous weather within an extra-tropical cyclone is dependent on its
structure, with high precipitation typically occurring at the location of weather fronts (Bjerknes, 1919; Dacre, 2020), and high
low-level wind speeds occurring at the locations of low-level conveyor belts and features such as sting jets (Browning,
30 1997, 2004; Martínez-Alvarado et al., 2014; Schultz and Browning, 2017).

In addition to the Norwegian Cyclone Model, the Shapiro-Keyser Model describes an alternative cycle of structural
development of extra-tropical cyclones (Shapiro and Keyser, 1990). The initial stages of each model are similar, but the
Shapiro-Keyser Model describes how extra-tropical cyclones may undergo frontal fracture during their mature phase and
develop a warm core (Shapiro and Keyser, 1990). Alternatively, the Norwegian Cyclone Model describes how extra-tropical
35 cyclones may continue to undergo occlusion during their mature phase, where the cold air mass wraps around the cyclone
centre into the warm air mass (Bjerknes, 1919, 1922). Case studies of past extra-tropical cyclones have been identified that
appear to follow a similar structural development cycle described in each model (e.g., Carlson, 1980; Browning, 2004), and it
is generally agreed that a particular extra-tropical cyclone may follow either models, or even a combination of both (Schultz
et al., 1998).

40 It is currently unclear whether Arctic cyclones have a similar cycle of structural development to extra-tropical cyclones.
The analysis of some individual Arctic summer cyclones suggests that they may have a different structure to extra-tropical
cyclones (Tanaka et al., 2012; Aizawa et al., 2014; Aizawa and Tanaka, 2016; Tao et al., 2017). Aizawa and Tanaka (2016)
showed that the Great Arctic Cyclone of 2012 developed an axi-symmetric cold core and barotropic structure during its mature
phase, which contrasts with the Norwegian Cyclone Model (Bjerknes, 1919, 1922) and the Shapiro-Keyser Model (Shapiro
45 and Keyser, 1990). This unique structure is also identified in two other past Arctic cyclones that occurred in June 2008 (Aizawa
et al., 2014; Aizawa and Tanaka, 2016) and September 2010 (Tao et al., 2017). Tao et al. (2017) showed that in their case study,
a lower stratospheric positive potential vorticity anomaly played a decisive role in that cyclone's development. However, a
more systematic study that examines a greater sample of Arctic cyclones is required to show this unique cyclone structure in
generality.

50 Some Arctic cyclones have also been found to have exceptionally long lifetimes, potentially causing prolonged hazardous
weather in the Arctic (Simmonds and Rudeva, 2012; Aizawa and Tanaka, 2016; Tao et al., 2017). Cyclones are associated with
rough sea conditions including high surface wind speeds and high ocean waves (Thomson and Rogers, 2014; Liu et al., 2016;
Waseda et al., 2018). Arctic cyclones can also break-up sea ice, which may then become mobile and drift toward shipping lanes,
creating an additional hazard (Simmonds and Keay, 2009; Asplin et al., 2012; Parkinson and Comiso, 2013; Peng et al., 2021).
55 Simmonds and Rudeva (2012) showed that the Great Arctic Cyclone of 2012 had a lifetime greater than 10 days. Moreover,
the June 2008 case study from Aizawa and Tanaka (2016) had a lifetime that was greater than 14 days. It is currently uncertain
how typical these longer-lived Arctic cyclones are.

Previous research on the structure and development of Arctic cyclones has primarily focused on case studies occurring in
summer (Tanaka et al., 2012; Aizawa et al., 2014; Aizawa and Tanaka, 2016; Tao et al., 2017). But the spatial distribution



60 of Arctic cyclones has been found to vary seasonally (Reed and Kunkel, 1960; Serreze et al., 2001; Simmonds et al., 2008; Crawford and Serreze, 2016; Vessey et al., 2020). In winter, Arctic cyclone track density is typically highest over the Greenland, Norwegian and Barents Seas and over the Canadian Archipelago, whereas in summer, Arctic cyclone track density is typically highest over the coastline of Eurasia and the Arctic Ocean (Vessey et al., 2020). The impact of the environmental conditions on the development of Arctic cyclones during winter and summer is an open question.

65 This study aims to describe the typical lifetime, structure, and development of a large sample of past intense winter (DJF) and summer (JJA) Arctic cyclones, using a storm compositing methodology. The focus is on intense cyclones that would most endanger human activity. Winter extra-tropical cyclones occurring over the North-Atlantic Ocean are used as a reference to compare with intense winter and summer Arctic cyclones, as they have been investigated more extensively in previous research (e.g., Bjerknes, 1919, 1922; Shapiro and Keyser, 1990; Browning, 1997, 2004; Catto et al., 2010). The aim of this study will
70 be achieved by answering the following questions:

- What are the typical lifetimes of intense winter and summer Arctic cyclones?
- How does the composite structure of intense winter and summer Arctic cyclones develop before and after the time of maximum intensity?
- How does the lifetime and composite structure of intense winter and summer Arctic cyclones differ to that of intense
75 North-Atlantic Ocean extra-tropical cyclones?

This paper continues in Section 2, where the methods used in this study are described. This includes a description of the data, storm tracking method and storm compositing method used. Results are then described in Section 3, detailing the typical lifetimes, spatial distribution and composite structure of intense synoptic-scale winter and summer Arctic cyclones and winter North Atlantic Ocean extra-tropical cyclones. Finally, a summary of the main conclusions is given in Section 4.

80 2 Methodology

2.1 Data

This study uses data from the European Centre for Medium-Range Weather Forecasts (ECWMF) fifth generation atmospheric reanalysis (ERA5) (Hersbach et al., 2020). Reanalysis datasets provide spatially and temporally homogeneous datasets, which combine past observations of the atmosphere with current atmospheric models to produce the best approximation of past
85 atmospheric states. ERA5 is the latest and highest resolution reanalyses to be produced by the ECMWF.

ERA5 includes global atmosphere data from 1979 - present. Data is output at a horizontal resolution of approximately 31 km (or TL639), with 137 levels up to 0.01 hPa. Historical observations are quality controlled and assimilated into the ECMWF IFS (41r2) model using a 4D variational data assimilation scheme to create a best approximation of the past atmosphere. From ERA5, the surface mean sea level pressure (MSLP) field, and the temperature, wind (u-component and v-component), vertical



90 velocity, relative humidity, and potential vorticity fields over nine pressure levels (925 hPa, 850 hPa, 700 hPa, 600 hPa, 500 hPa, 400 hPa, 300 hPa, 200 hPa and 100 hPa) are used at 6-hour time intervals (00:00, 06:00, 12:00 and 18:00).

2.1.1 Storm tracking

Cyclones are identified in ERA5 using the storm tracking algorithm developed by Hodges (1994, 1995, 1999). Vessey et al. (2020) showed that storm tracking based on 850 hPa relative vorticity generally identifies more Arctic cyclones than those based on MSLP. Therefore, Arctic cyclones in this study are identified as maxima in the 850 hPa relative vorticity field. This field is first spectrally truncated to a spectral resolution of T42 and is filtered to remove the planetary scales for total wavenumbers less than or equal to 5. This ensures that synoptic-scale systems that are independent of large-scale forcings are focused upon.

Cyclones are then identified as maxima in the 850 hPa relative vorticity field at each timestep. Features are then grouped into cyclone tracks using a nearest-neighbour approach, which links feature points in consecutive time-steps. Once all cyclone tracks have been identified in ERA5 from 1979 - 2020, they are then filtered to retain cyclones that last more than 2 days and travel more than 1000 km. This further ensures that synoptic-scale and mobile cyclones are focused upon. Arctic cyclones are defined in this study as any cyclone that travels north of 65°N. For comparison, Arctic cyclones are contrasted with extra-tropical winter cyclones that occurred over the North Atlantic Ocean.

2.2 Storm compositing

105 The structure of cyclones is examined using a system centred composite method, which is described in Bengtsson et al. (2007, 2009) and Catto et al. (2010). A composite method can identify the general structure of a group of cyclones, by taking an average of atmospheric fields across a space centred on each cyclones centre. A composite is the average structure of multiple cyclones. It allows for the identification of the general structure of a group of cyclones, but without smaller scale features that tend to be smoothed out by the method. The composite method has three steps: storm selection, storm rotation and lifetime positioning.

115 Firstly, the 100 most intense winter North Atlantic Ocean extra-tropical cyclones and Arctic winter and summer cyclones with the lowest MSLP minima between 1979 and 2020 in ERA5 are identified (storm selection). To be characterised as an Arctic cyclone, cyclones must have 60% of their track points in the Arctic (north of 65°N) and their maximum intensity (i.e., minimum MSLP) in the Arctic. This is to ensure that intense Arctic cyclones that spend most of their lifetime in the Arctic are selected. A similar procedure was followed to identify the 100 most intense cyclones that occurred over the North Atlantic Ocean region, between -53 to 20°E and 30 - 65°N, from 1979 - 2020.

120 The atmospheric fields associated with each cyclone are then sampled onto a 20° longitude-latitude rectangular grid with a horizontal resolution of 0.5°, so that the origin 0,0 is centred on the cyclone centre (the point of minimum MSLP). This grid is initially setup to be centred on the equator and ensures a fair spatial comparison between cyclones that occur at different latitudes. This grid can then be rotated so that each cyclone can be orientated according to the cyclone's propagation direction, or the geographical orientation of each cyclone is kept before an average can be made over all cyclones (storm rotation).



Both approaches of storm rotation have been used in previous research (e.g., Wang and Rogers, 2001; Bauer and Del Genio, 2006; Bengtsson et al., 2007, 2009; Catto et al., 2010). An advantage of rotating each cyclone to a common direction (e.g., propagation direction) before averaging is that system-relative winds can be determined, which are independent of the cyclones
125 propagation velocity. This can help to determine features such as conveyor belts within the composite (Catto et al., 2010). In this study, cyclone composites are produced by rotating each cyclone to a common direction of propagation before averaging, so that it can be determined whether conveyor belts, which have been shown to occur in typical extra-tropical cyclones (Browning, 1997), also occur in Arctic cyclones.

Composites are then produced by taking an average of the atmospheric fields around the cyclone centre at various points in
130 each cyclone's lifecycle (lifetime positioning). Composites in this study are produced at the time of maximum intensity, when each cyclone reaches their MSLP minima. This is to determine the structure of cyclones when they are at their most hazardous. The development of each composite is also determined at time-steps up to 48 hours before and up to 192 hours after the time of maximum intensity at 48-hour intervals. Temperature anomalies are calculated by subtracting the temperature value at each spatial point from the mean temperature across the horizontal 20° longitude-latitude domain at each vertical level.

135 3 Results

3.1 Cyclone Lifetime

The 100 most intense winter and summer Arctic cyclones are typically less intense than the 100 most intense North Atlantic Ocean winter extra-tropical cyclones (see Figure 1a). The mean minimum MSLP of the 100 most intense North Atlantic Ocean winter extra-tropical cyclones is 945.5 hPa but is 953.8 hPa and 974.6 hPa for the 100 most intense Arctic winter and summer
140 cyclones respectively. The mean lifetime of the 100 most intense Arctic summer cyclones is however much greater than that of winter Arctic cyclones and North Atlantic Ocean extra-tropical cyclones (see Figure 1).

The mean lifetime of the 100 most intense Arctic summer cyclones (9.7 days) is more than 3 days greater than that of the 100 most intense Arctic winter cyclones (6.1 days) and more than 4 days greater than that of the 100 most intense North Atlantic Ocean winter extra-tropical cyclones (5.4 days) (see Figure 1a). This is also shown by more of the 100 most intense Arctic
145 summer cyclones existing longer before and after their time of maximum intensity (see Figure 1a). The modal lifetime of the 100 most intense Arctic summer cyclones is also greater than 10 days, with just under half of these cyclones (44) surpassing this threshold (see Figure 1b). This is much greater than the modal lifetime of the 100 most intense winter Arctic and North Atlantic Ocean extra-tropical cyclones (4-6 days). With a longer lifetime, Arctic summer cyclones may cause prolonged hazardous weather conditions in the Arctic, such as high wind and waves (Thomson and Rogers, 2014; Liu et al., 2016; Waseda et al.,
150 2018).

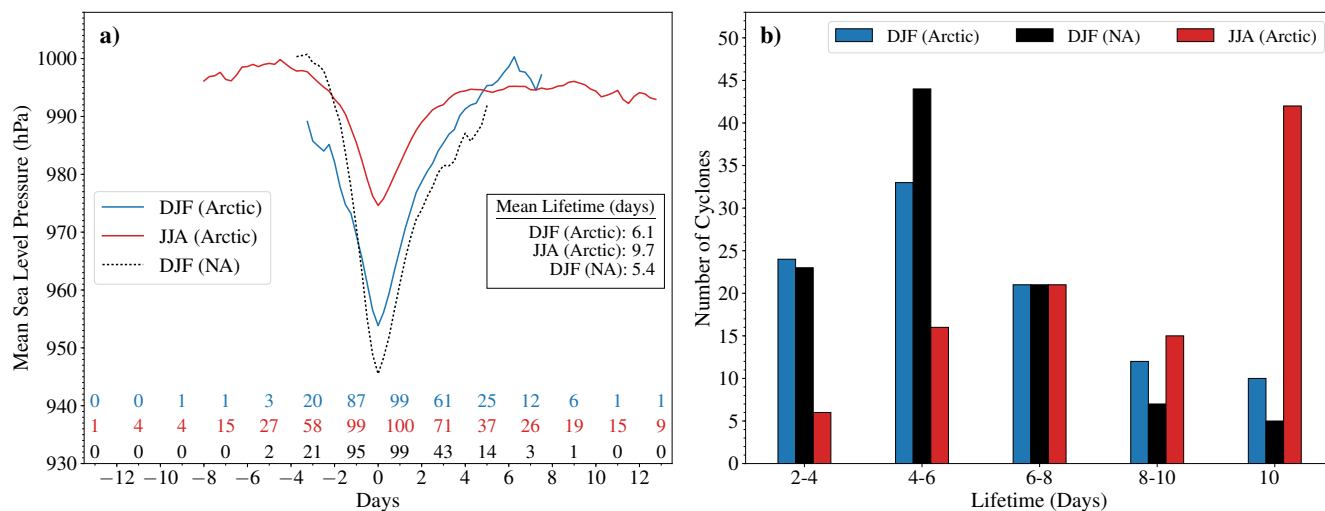


Figure 1. Life-cycles of the 100 most intense winter (DJF) and summer (JJA) Arctic cyclones and winter North Atlantic (NA) Ocean extra-tropical cyclones between 1979 and 2020. **a)** The mean composite life-cycle development in intensity (MSLP), when cyclones are centred at the time of their maximum intensity (minimum MSLP) and where at least 10 cyclones exist at each time interval. The numbers indicate how many cyclones exist at each time interval. **b)** The distribution in the lifetimes of the 100 most intense winter and summer Arctic cyclones and winter North Atlantic (NA) Ocean extra-tropical cyclones.

3.2 Arctic cyclone spatial distribution

The track density of Arctic cyclones has been found in previous research to vary seasonally (Reed and Kunkel, 1960; Serreze et al., 2001; Simmonds et al., 2008; Crawford and Serreze, 2016; Vessey et al., 2020). Arctic cyclone track density is typically highest in winter over the Greenland, Norwegian and Barents Seas, and over the Canadian Archipelago, whereas in summer, Arctic cyclone track density is typically highest over the coastline of Eurasia and the Arctic Ocean (Vessey et al., 2020). This is reflected in the spatial distribution of the locations of maximum intensity of the 100 most intense Arctic winter and summer cyclones (see Figure 2). Generally, the 100 most intense winter Arctic cyclones have their maximum intensity over the Greenland, Norwegian and Barents Seas (see Figure 2). In contrast, the 100 most intense Arctic summer cyclones tend to have their maximum intensity over higher latitudes and over the Arctic Ocean that is north of the Eurasia coastline and the Bering Strait (see Figure 2).

3.3 Horizontal composite structure at the time of maximum intensity

The 100 most intense summer Arctic cyclones are less intense than winter Arctic and North Atlantic Ocean extra-tropical cyclones (see Figure 1). Thus, the minimum MSLP of the Arctic summer cyclone composite at the time of maximum intensity (976.6 hPa) is higher than the winter Arctic cyclone (958.8 hPa) and North Atlantic Ocean extra-tropical cyclone (949.2 hPa) composites (see Figure 3a, 3d, and 3g). The pressure gradients are tighter in the Arctic winter cyclone composite than in

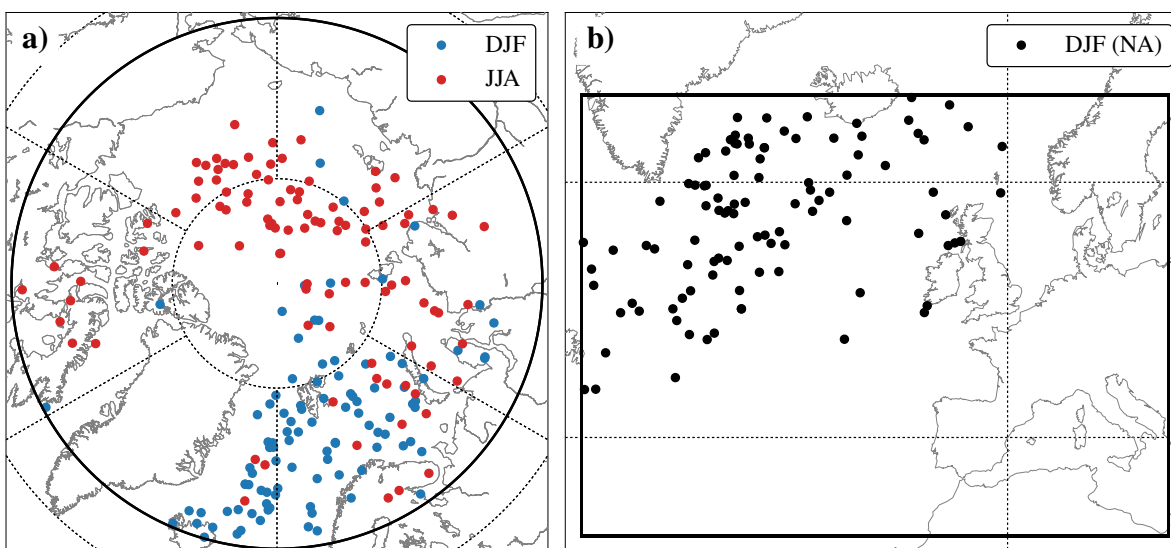


Figure 2. The locations of the points of maximum intensity (minimum MSLP) of each of the 100 most intense **a**) winter (DJF) and summer (JJA) Arctic cyclones and **b**) winter North Atlantic (NA) Ocean extra-tropical cyclones between 1979 and 2020. Longitudes are shown every 60°E, and latitudes are shown at **a**) 80°N, 65°N (bold) and 50°N, and **b**) 60°N and 40°N, with the thick black lines indicating the domains used for selecting each class of cyclone.

the Arctic summer cyclone composite, but tightest in the North Atlantic Ocean winter extra-tropical cyclone composite. The Arctic summer cyclone composite is also smaller than the Arctic winter and North Atlantic Ocean cyclone composites. This is shown by the 1000 hPa contour not exceeding a distance of 1100 km from the Arctic summer cyclone composite centre, but exceeding this threshold in the winter Arctic and North Atlantic Ocean extra-tropical cyclone composites (see Figure 3a, 3d, and 3g). Moreover, the Arctic summer cyclone composite is more axi-symmetric than the winter Arctic and North Atlantic Ocean extra-tropical cyclone composites (see Figure 3a, 3d, and 3g), which have tighter pressure gradients south of the composite cyclone centre than north of the composite cyclone centre.

The maximum 850 hPa earth-relative wind speeds are weaker in the Arctic summer cyclone composite (20.9 m s^{-1}) than the Arctic winter cyclone composite (24.5 m s^{-1}) and the North Atlantic Ocean winter extra-tropical cyclone composite (32.3 m s^{-1}) (see Figure 3b, 3e and 3h). This is likely a consequence of the weaker pressure gradients within the Arctic summer cyclone composite. The area where the 850 hPa earth-relative wind speeds exceed 10 m s^{-1} is also much greater in the Arctic winter and North Atlantic Ocean extra-tropical cyclone composites than the Arctic summer cyclone composite (see Figure 3b, 3e and 3h). In each cyclone composite, the maximum 850 hPa earth-relative wind speeds occur in the southern region of the composite and near the composite centre (see Figure 3b, 3e and 3h). In this region, the system-relative winds would be enhanced by the cyclonic (anti-clockwise) propagation velocity of the cyclone.

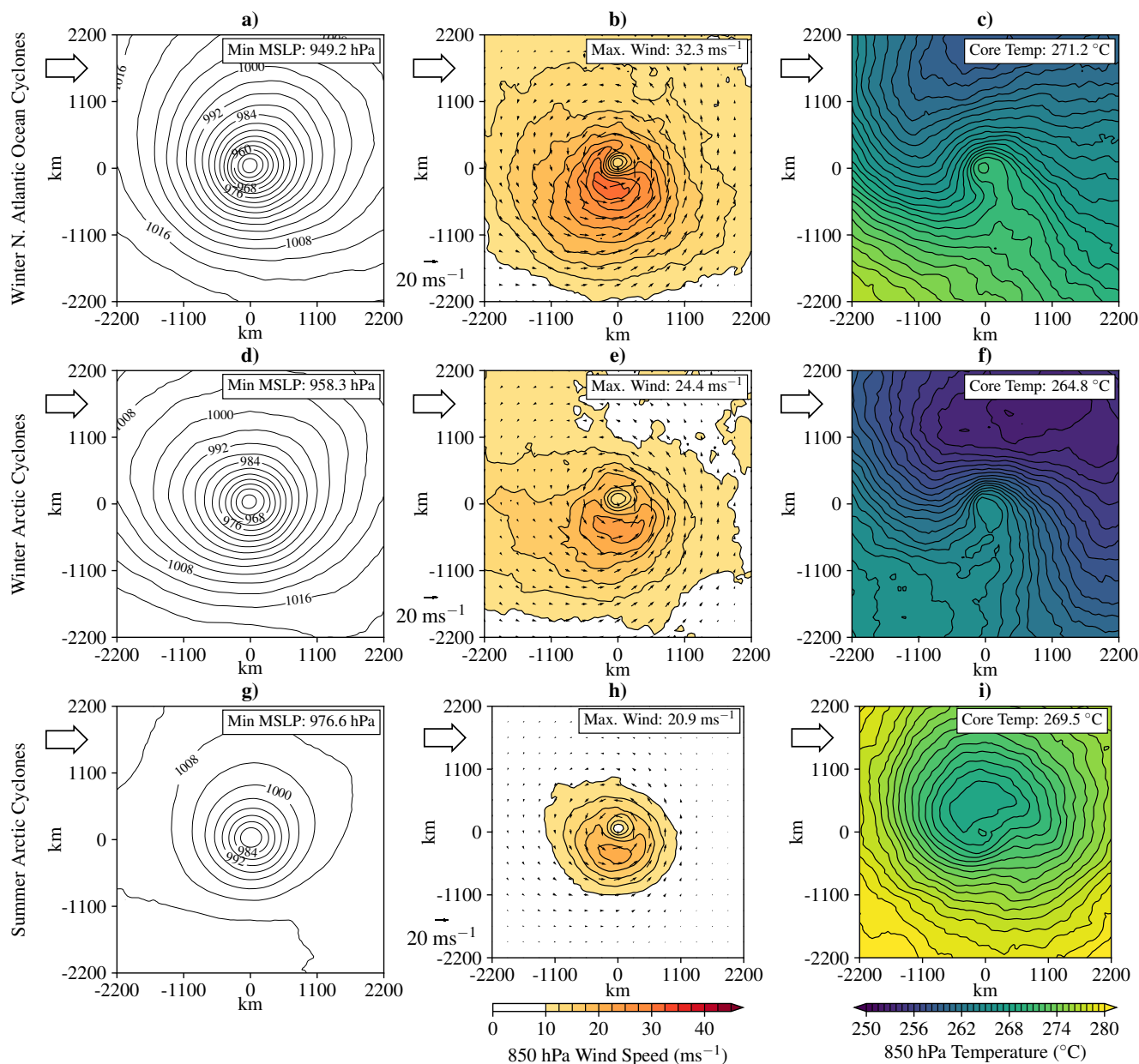


Figure 3. Horizontal mean sea level pressure (MSLP) (hPa) (left panel), 850 hPa earth-relative wind speed (m s^{-1}) (middle panel) and 850 hPa temperature ($^{\circ}\text{C}$) (right panel) composite structure at the time of maximum intensity (minimum MSLP), of winter (DJF) North Atlantic Ocean extra-tropical cyclones (top panel), winter Arctic cyclones (middle panel), and summer (JJA) Arctic cyclones (bottom panel). The large arrow indicates the direction of storm propagation.



Despite similarities in the spatial distribution of the 850 hPa earth-relative winds within each composite, the 850 hPa temperature structure of the Arctic summer cyclone composite is different to that of the winter Arctic and North Atlantic Ocean extra-tropical cyclone composites (see Figure 3c, 3f and 3i). At the time of maximum intensity, the Arctic summer cyclone composite is characterised by a cold core at the centre of the composite (see Figure 3i). In contrast, the Arctic winter and North Atlantic Ocean extra-tropical cyclone composites are characterised by high temperature gradients between the warm air to the south and cold air to the north of the composite cyclone centres (see Figure 3c and 3f). These divisions between warm and cold air would be associated with the location of weather fronts. The winter Arctic and North Atlantic Ocean extra-tropical cyclone composites also show signs that cold air has started to occlude into the warm air around the composite cyclone centre.

The 850 hPa temperature structure of the Arctic summer cyclone composite is different to that of winter Arctic cyclones and North Atlantic Ocean winter extra-tropical cyclones. It is also different to that described in the Norwegian Cyclone Model and Shapiro-Keyser Model (Bjerknes, 1919, 1922; Shapiro and Keyser, 1990). This contrasts with results from Clancy et al. (2022), who show that the structure of Arctic cyclones in every season is comparable to those in the mid-latitudes. However, Clancy et al. (2022) used a different cyclone compositing methodology, storm tracking algorithm and did not filter Arctic cyclones to retain the 100 most intense cyclones, instead calculating the cyclone composite as an average of many more cyclones per season.

3.4 Vertical composite structure at the time of maximum intensity

Cyclones typically contain conveyor belts, which are distinct airstreams occurring in different regions and altitudes within a cyclone (Browning, 1997; Catto et al., 2010; Dacre et al., 2012). These include a warm conveyor belt (WCB) that is typically located in front of the cold front and ascends from south to north parallel to the front. The WCB typically rises above the cold conveyor belt (CCB), which typically occurs at low-levels in the atmosphere and wraps around the cyclone centre to the north (Browning, 1997).

The ascent of air associated with the WCB is shown in the winter North Atlantic Ocean extra-tropical cyclone and the Arctic winter cyclone composites ahead of the cyclone centre where the cold front would be typically located (see Figure 4a, 4b and 4c). This suggests that a WCB may be present within each composite. In the Arctic summer cyclone composite, the magnitude of ascent shown in the vertical velocity composite is much weaker than in the winter North Atlantic Ocean extra-tropical cyclone and Arctic cyclone composites (see Figure 4). The maximum vertical velocity in the winter North Atlantic Ocean extra-tropical cyclone composite is 28.7 hPa h^{-1} , 17.2 hPa h^{-1} in the Arctic winter cyclone composite, and 9.6 hPa h^{-1} in the Arctic summer cyclone composite (see Figure 4). This suggests that the WCB may be less well defined in Arctic summer cyclones.

The 400 hPa relative humidity composites for each class of cyclone show that the Arctic summer cyclone composite is more axi-symmetric than the winter North Atlantic Ocean extra-tropical cyclone composite and the Arctic winter cyclone composite (see Figure 4d, 4e and 4f). High values of relative humidity are more confined around the composite cyclone centre to the north and east in both of the North Atlantic Ocean extra-tropical cyclone and Arctic winter cyclone composites, perhaps indicating

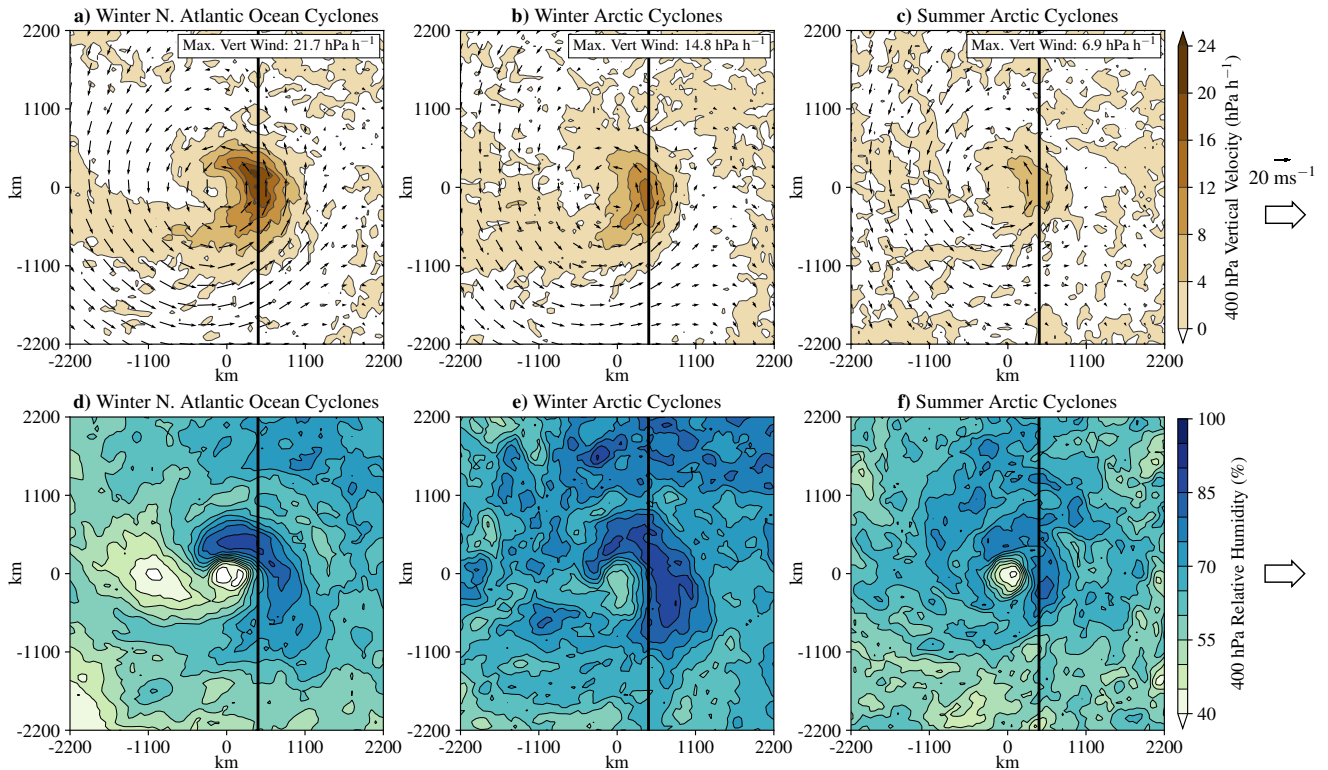


Figure 4. Horizontal 400 hPa system relative winds (m s^{-1}) (quivers) and vertical velocity (hPa h^{-1}) (contours) (top panel), and 400 hPa relative humidity (%) (bottom panel) composite structure at the time of maximum intensity (minimum MSLP), of winter (DJF) North Atlantic Ocean extra-tropical cyclones (left panel), winter Arctic cyclones (middle panel), and summer (JJA) Arctic cyclones (right panel). Positive values of vertical velocity indicate ascent. The large arrow indicates the direction of storm propagation. The transect (bold line) from south to north 4° degrees ahead of the composite cyclone centre and perpendicular to the cyclones direction of propagation indicates the vertical slice used to produce Fig. 5.

215 where moisture has risen from the surface within the cyclone at the typically location of weather fronts. West of the composite cyclone centre, drier air is shown at the 400 hPa level in the North Atlantic Ocean extra-tropical cyclone composite that appears to be intruding towards the composite cyclone centre, perhaps indicating the presence of a dry intrusion. But this feature is less pronounced in the winter and summer Arctic cyclone composites.

By analysing the transect 4° degrees ahead of cyclone centre and perpendicular to the cyclones direction of propagation that
 220 intersects the maximum in vertical velocity in each composite and where the WCB is indicated to occur (see Figure 4), the WCB and CCB appear to be present in both the winter Arctic and North Atlantic Ocean cyclone composites (see Figure 5a and 5b). The CCB is shown by the low-level high magnitude system-relative zonal (U-component) wind speeds within the vertical cross section, which occur approximately 550 km north of the level of the composite cyclone centre. The magnitude of the

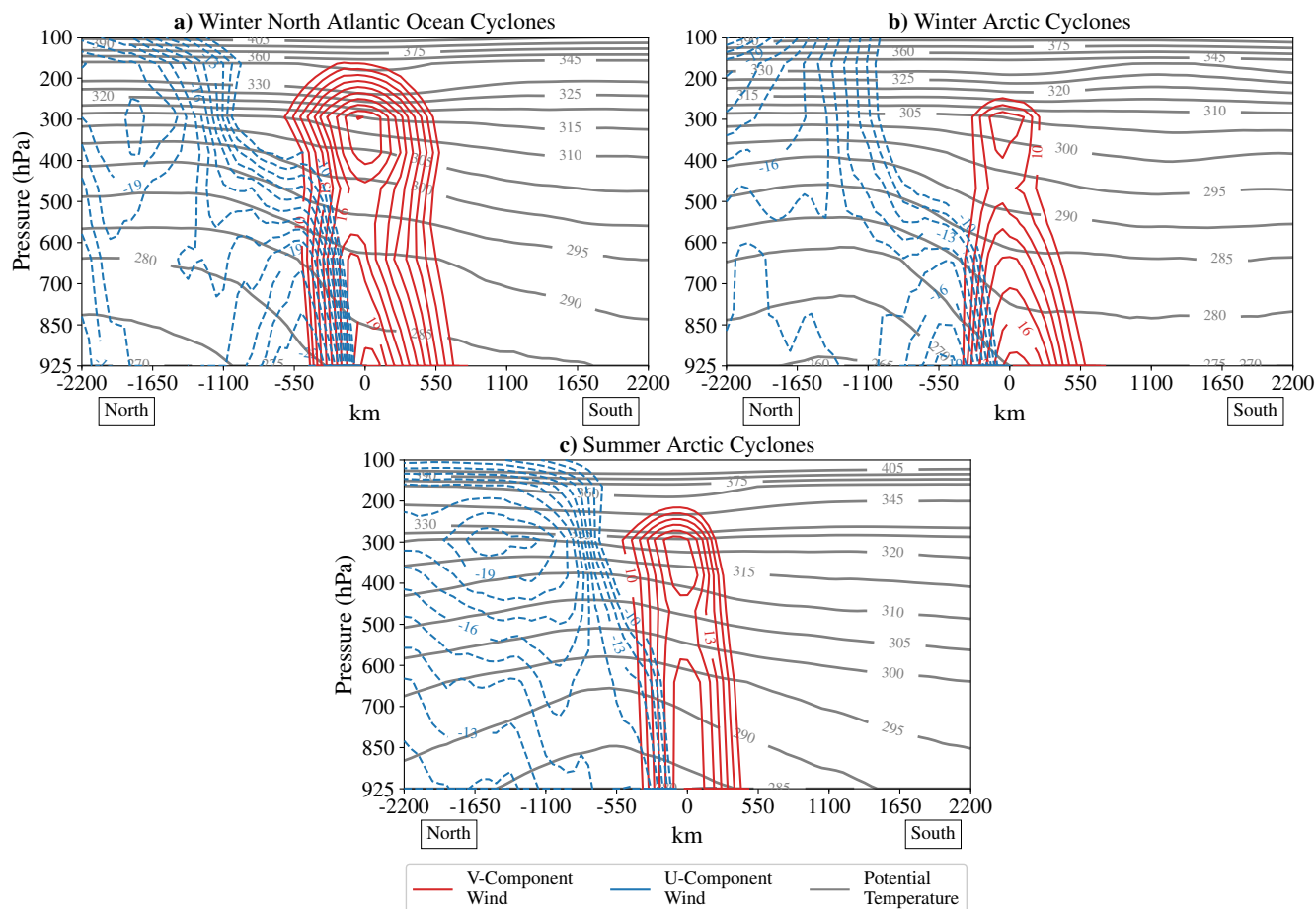


Figure 5. Composite vertical slices through the transect perpendicular to the direction of cyclone propagation and 4° ahead of the composite cyclone centre (see Figure 4), of **a)** winter (DJF) North Atlantic Ocean extra-tropical cyclones, **b)** winter Arctic cyclones, and **c)** summer (JJA) Arctic cyclones. Red contours (shown every 1 m s^{-1} from 10 m s^{-1}) show the V-component (meridional) winds, blue contours (shown every 1.0 m s^{-1} below -10 m s^{-1}) show the U-component (zonal) winds and grey contours (shown every 5° C up to 330° C and then every 15° C) show potential temperature isentropes.

zonal winds of the CCB are lower in the Arctic winter cyclone composite (approximately 18 m s^{-1}) than the North Atlantic Ocean winter cyclone composite (approximately 22 m s^{-1}).

The WCB is shown in the winter Arctic and North Atlantic Ocean cyclone composites by the high magnitude meridional (V-component) system-relative winds within the vertical cross section, which occur south of the CCB and between 925hPa to 600 hPa (see Figure 5a and 5b). Like the CCB, the maximum magnitude of these meridional wind speeds is lower in the Arctic winter cyclone composite (approximately 18 m s^{-1}) than the North Atlantic Ocean winter cyclone composite (approximately 20 m s^{-1}). The spatial distribution of the system-relative wind speeds in these composites is similar to that shown by Catto et al.



(2010), who showed the composite structure of the 50 most intense North Atlantic and Pacific Ocean extra-tropical cyclones, using the ERA-40 reanalyses. The stark changes in the wind direction shown north of the level of the cyclone composite centre in each cross section of the winter North Atlantic Ocean cyclone and Arctic cyclone composites indicates the presence of the CCB and WCB in each composite.

235 Differences are shown in the vertical structure of the system-relative winds within the summer Arctic cyclone composite when compared to the winter Arctic and North Atlantic Ocean extra-tropical cyclone composites. There are high magnitude meridional (V-component) winds shown ahead of the cyclone composite centre where the potential temperature isentropes ascend, suggesting the presence of the WCB (see Figure 5c). But in the Arctic summer cyclone composite, the highest zonal wind speeds north of the cyclone composite centre do not occur at the surface (see Figure 5c). Instead, the highest zonal wind
240 speeds occur at the 300 hPa level approximately 1600 km from the cyclone composite centre. This suggests that the CCB, which typically occurs near the surface, is less well defined in summer Arctic cyclones.

The distribution of the potential temperature isentropes within the Arctic summer cyclone composite cross section also differs to that of winter Arctic and North Atlantic Ocean extra-tropical cyclones (see Figure 5). In contrast, the slope of the potential temperature isentropes reverses north of the composite cyclone centre, where the isentropes ascend but then descend
245 south to north along this cross section (see Figure 5c). At the time of maximum intensity, Arctic summer cyclones have developed a cold core (see Figure 3), which could contribute to this distribution in the isentropes.

3.5 Development in the horizontal composite structure

The 700 hPa temperature structure of the winter North Atlantic Ocean extra-tropical cyclone composites and the winter and summer Arctic cyclone composites 48 hours before the time of maximum intensity is similar, with each cyclone developing in
250 a region of high temperature gradients (see Figure 6). This is similar to the Polar Front described by Bjerknes (1919, 1922). Temperature gradients within the winter North Atlantic Ocean extra-tropical cyclone and Arctic cyclone composites are much greater than that of the summer Arctic cyclone composite. This is likely because intense winter Arctic cyclones also tend to develop over the North Atlantic Ocean (see Figure 2, where meridional temperature gradients and baroclinicity are high, especially in winter. However, from the time of maximum intensity, the development in the Arctic summer cyclone composite
255 differs to that of the winter North Atlantic Ocean extra-tropical cyclone and Arctic cyclone composites.

From the time of maximum intensity, the Arctic summer cyclone composite develops a cold core centre that becomes more defined and colder (see Figures 6i and 7). The temperature anomaly at the composite cyclone centre at the time of maximum intensity is $-3.8\text{ }^{\circ}\text{C}$ (see Figure 6h), but lowers to $-8.7\text{ }^{\circ}\text{C}$ and $-10.6\text{ }^{\circ}\text{C}$ 48 and 144 hours after the time of maximum intensity (see Figures 6i and 7b). This shows that Arctic summer cyclones tend to develop a cold core centre around the time of maximum
260 intensity and retain this structure until they dissipate.

This is in contrast with the winter Arctic and North Atlantic Ocean extra-tropical cyclone composites that appear to follow the process of occlusion, where cold air wraps around the composite centre (see Figure 6). This structural transition of the Arctic summer cyclone composite is also different to the Norwegian Cyclone Model (Bjerknes, 1919, 1922), where cyclones

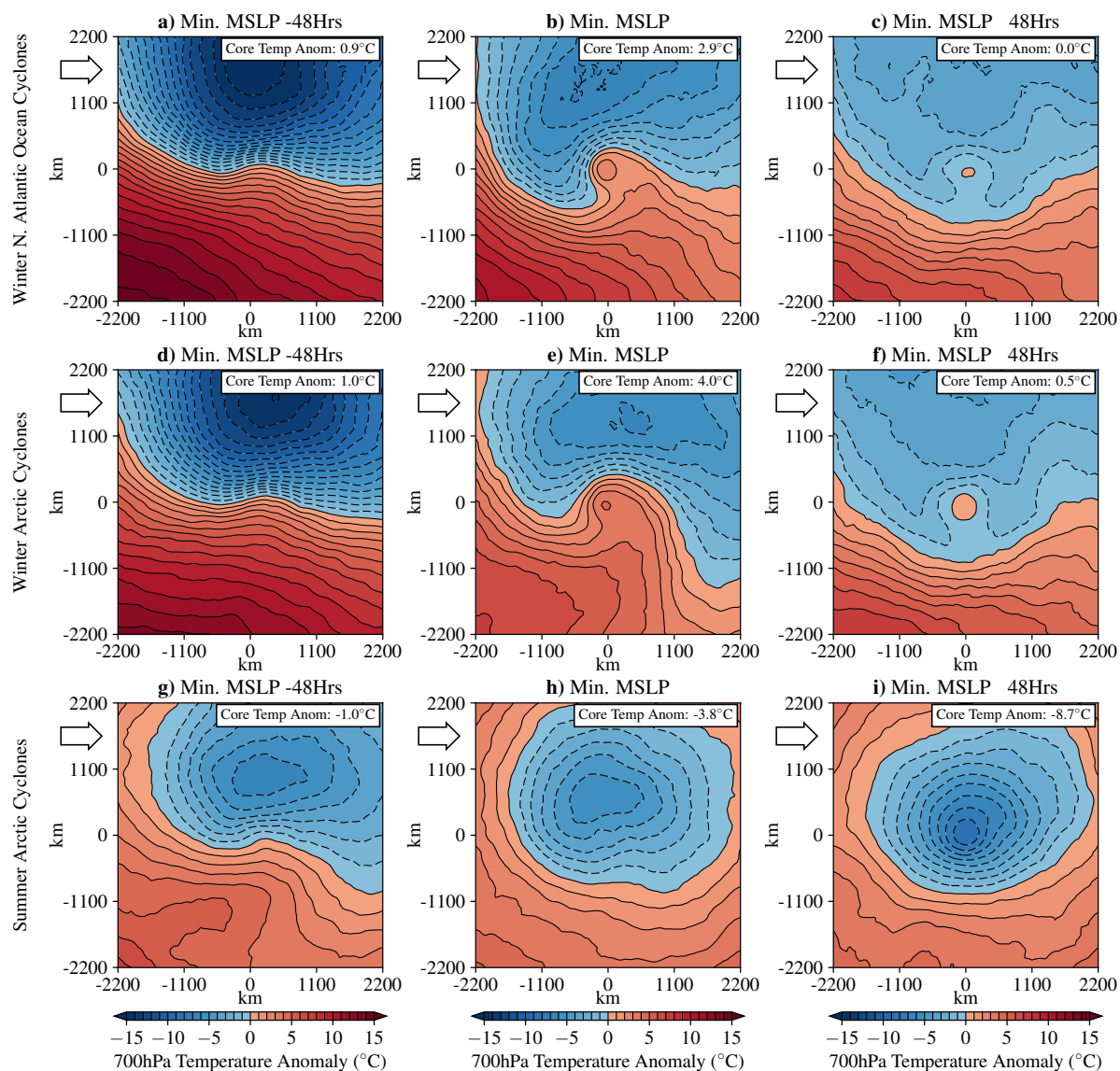


Figure 6. Horizontal 700 hPa temperature anomaly ($^{\circ}\text{C}$) composite structure 48 hours before the time of maximum intensity (minimum MSLP) (left panel), **b**) at the time of maximum intensity (middle panel), and 48 hours after the time of maximum intensity (right panel), of winter (DJF) North Atlantic Ocean extra-tropical cyclones (top panel), winter Arctic cyclones (middle panel), and summer (JJA) Arctic cyclones (bottom panel). The large arrow indicates the direction of storm propagation.

265 tend to undergo occlusion, and the Shapiro-Keyser Model (Shapiro and Keyser, 1990), where cyclones tend to undergo frontal fracture and develop a warm core centre.

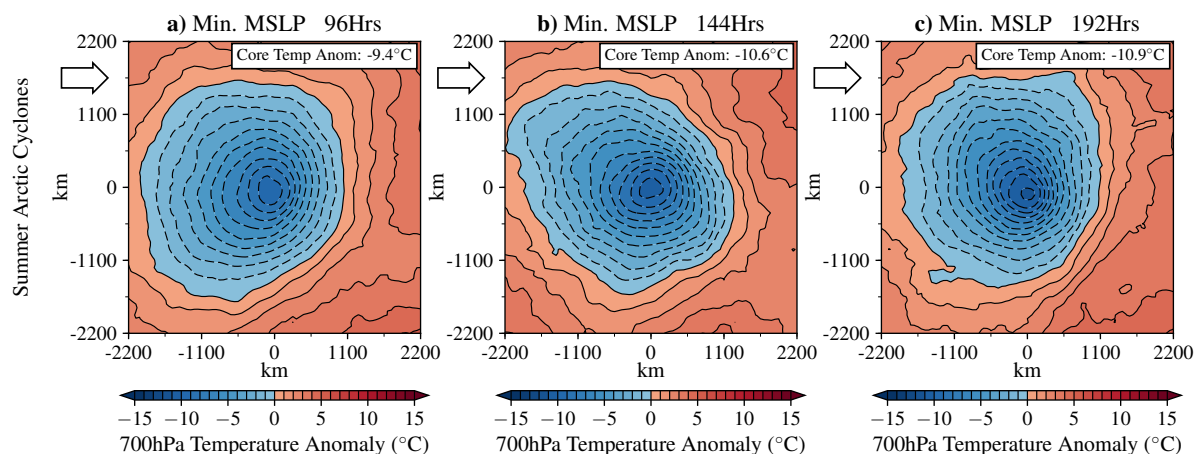


Figure 7. Horizontal 700 hPa temperature anomaly ($^{\circ}\text{C}$) composite structure 96 (left), 144 (middle) and 192 (right) hours after the time of maximum intensity (minimum MSLP) of summer (JJA) Arctic cyclones. The large arrow indicates the direction of storm propagation.

3.6 Development in the vertical composite structure

The unique structural transition in temperature of the Arctic summer cyclone composite is also shown throughout the vertical extent of the composite (see Figure 8). From the time of maximum intensity, cold air in the Arctic summer cyclone composite intrudes through the centre of the composite, which ultimately leads to the composite to develop a cold core structure throughout the troposphere (see Figure 8g, 8h and 8i). This is similar to the structure found in the Great Arctic Cyclone of 2012, which was shown by Aizawa and Tanaka (2016).

The Arctic summer cyclone composite shows further differences to the winter North Atlantic Ocean extra-tropical and Arctic cyclone composites. The temperature anomaly in the stratosphere is much more defined and larger ($8.0 - 9.0^{\circ}\text{C}$) in the Arctic summer cyclone composite at and after the time of maximum intensity (see Figure 8h and 8i). In contrast, the maximum temperature anomaly in the stratosphere after the time of maximum intensity in the winter North Atlantic Ocean extra-tropical cyclone and Arctic cyclone composites is $5.0 - 6.0^{\circ}\text{C}$ (see Figure 8). Furthermore, the altitude of the tropopause is much lower in the Arctic summer cyclone composite at and after the time of maximum intensity than the winter North Atlantic Ocean extra-tropical cyclone and Arctic cyclone composites (see Figure 8). The level of tropopause is shown to be approximately 500 hPa at the centre of Arctic summer cyclone composite at the after the time of maximum intensity. In contrast, the level of tropopause is approximately 300 hPa at the centre of the winter North Atlantic Ocean extra-tropical cyclone and Arctic cyclone composites at and after the time of maximum intensity.

The vertical temperature structure of the Arctic summer cyclone composite is shown to be more axi-symmetric from the time of maximum intensity than the winter North Atlantic Ocean cyclone and winter Arctic cyclone composites (see Figure 8). This axi-symmetric structure after the time of maximum intensity is also shown in the system-relative wind speed fields (see Figure 9). After 48 hours from the time of maximum intensity, the Arctic summer cyclone composite develops system zonal

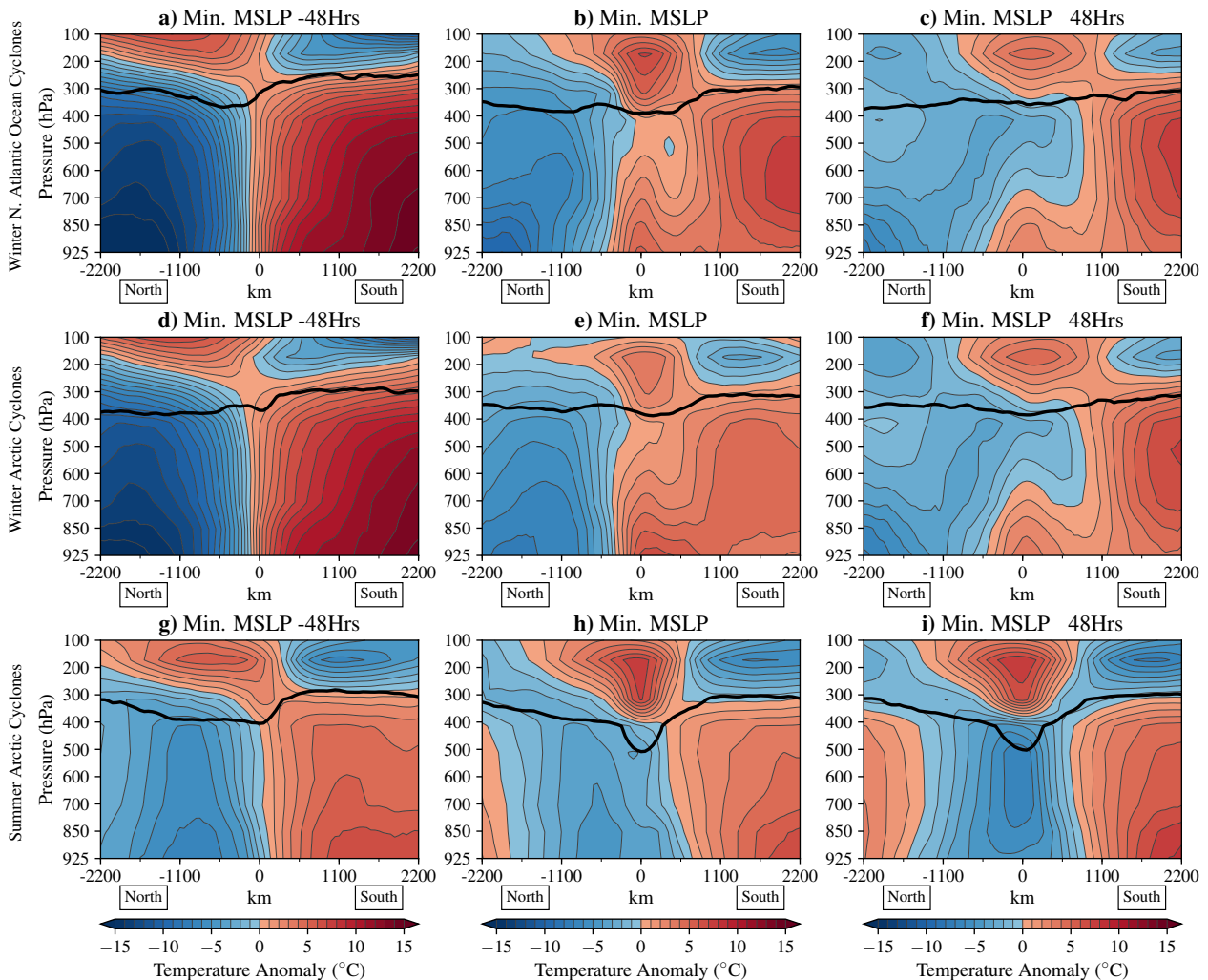


Figure 8. Vertical temperature anomaly ($^{\circ}\text{C}$) composite of winter (DJF) North Atlantic Ocean extra-tropical cyclones (top panel), winter Arctic cyclones (middle panel), and summer (JJA) Arctic cyclones (bottom panel), along the transect north to south through the composite cyclone centre, 48 hours before the time of maximum intensity (i.e., minimum MSLP) (left panel), at the time of maximum intensity (middle panel), and 48 hours after the time of maximum intensity (right panel). The thick black contour indicates the level of the tropopause (i.e., the 2PVU contour).

and meridional system-relative winds around the composite cyclone centre of similar magnitude (see Figure 9c and Figure 9f). Notably, system-relative winds are higher in the upper atmosphere than near the surface, where human activity would tend to occur.

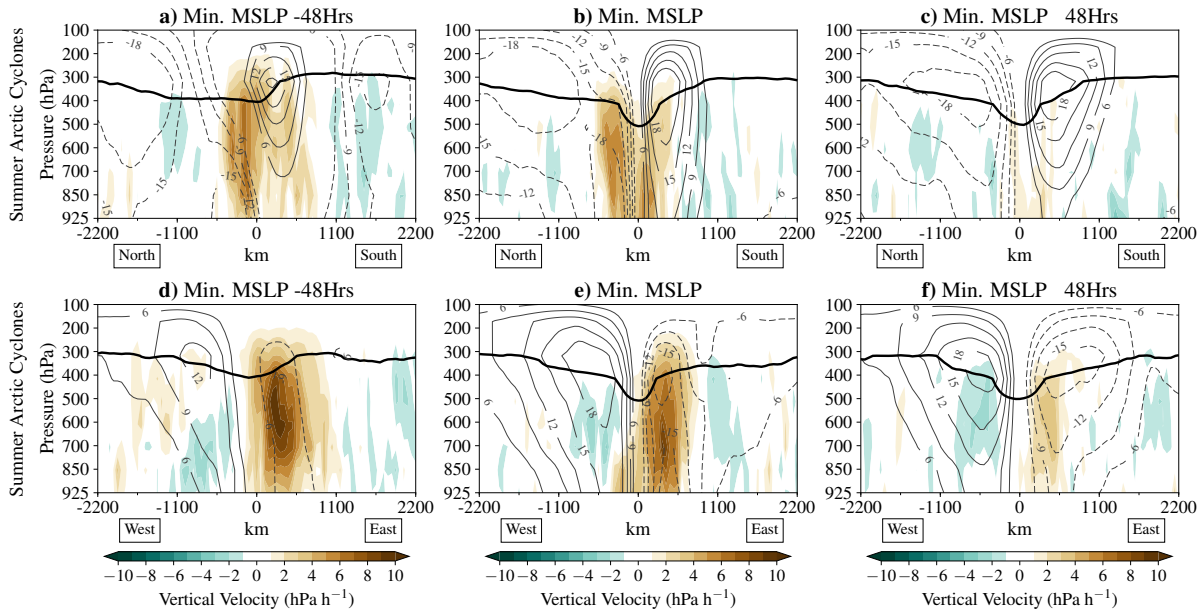


Figure 9. Vertical velocity (hPa h^{-1}) (colour) and system-relative (m s^{-1}) U-component (zonal) and V-component (meridional) wind speed (contours) composite structure of the 100 most intense summer (JJA) Arctic cyclones, along the transect north to south (top panel) and west to east (bottom panel) through the composite cyclone centre. Positive values of vertical velocity indicate ascent. Composites are shown 48 hours before the time of maximum intensity (i.e., minimum mean sea level pressure (MSLP) (left panel), at the time of maximum intensity (middle), and 48 hours after the time of maximum intensity (right panel). The thick black contour indicates the level of the tropopause (i.e., the 2PVU contour).

3.7 Comparison of the Arctic summer cyclone composite to the Aizawa and Tanaka (2016) model

290 Aizawa and Tanaka (2016) proposed a conceptual model of the structure of Arctic summer cyclones, based on just two past Arctic summer cyclone case studies. Here, the composite structure of the 100 most intense Arctic summer cyclones has been determined, allowing for the evaluation of the Aizawa and Tanaka (2016) conceptual model to the composite structure of a greater sample of past intense Arctic summer cyclones. This conceptual model highlights six main features of Arctic summer cyclones, which include: a warm core in the lower stratosphere and cold core in the troposphere, a deep tropopause fold descending down to 500 hPa over the cyclone centre, a secondary circulation in the troposphere, a downdraft in the lower stratosphere, a deep cyclonic circulation up into the stratosphere and a horizontal extent of approximately 5,000 km.

295 There are similarities between the Arctic summer cyclone composite and this conceptual model. The composite vertical structure of Arctic summer cyclones shows a warm anomaly in the lower stratosphere (up to 100 hPa) and a cold core throughout the troposphere (see Figure 8). There is also a deep tropopause fold that descends to 500 hPa shown in the Arctic summer cyclone composite (see Figure 8).

300



In contrast to the Aizawa and Tanaka (2016), the general size of the Arctic summer cyclone composite appears to be much less than 4,400 km (see Figure 3), as shown by the extent of the highest closed MSLP contour (1008 hPa). The Arctic summer cyclone composite from the time of maximum intensity also does not show a secondary circulation in the troposphere or deep cyclonic circulation into the stratosphere or a downdraft in the stratosphere (Figure 9). Before and after the time of maximum intensity, the Arctic summer cyclone composite does not show downdrafts (positive vertical velocity) on the outer flanks of the composite (see Figure 9). Only a weak ($< -3.0 \text{ hPa h}^{-1}$) downdrafts are shown in the composite before and at the time of maximum intensity (see Figure 9).

Overall, by analysing the composite structure of a large sample of past Arctic summer cyclones, there is evidence to support some aspects of the Aizawa and Tanaka (2016) conceptual model, which was based on the analysis of just two past Arctic cyclone case studies. Results from this study show that after the time of maximum intensity, intense Arctic summer cyclones do indeed likely have a warm core in the lower stratosphere and a cold core in the troposphere, and a deep tropopause fold descending into the troposphere over the cyclone centre. However, there is insufficient evidence to suggest that typical intense Arctic summer cyclones have a secondary circulation in the troposphere, a downdraft in the lower stratosphere, a deep cyclonic circulation up into the stratosphere and a horizontal extent of approximately 5,500 km (typical Arctic summer cyclones are likely smaller).

An aspect that is not considered by Aizawa and Tanaka (2016), but is highlighted in this study, is that intense Arctic summer cyclones appear to typically undergo a structural transition during their life-cycle. The development in the composite structure of intense Arctic summer cyclones shows that they undergo a transition from having a baroclinic structure to an axi-symmetric cold core structure throughout the troposphere around the time of maximum intensity. After this transition, the structure of intense Arctic summer cyclones is somewhat similar to the Aizawa and Tanaka (2016) model.

4 Summary and Conclusions

The location and intensity of hazardous weather within a cyclone is dependent on its development and structure. Previous analysis of individual past Arctic summer cyclones suggests that they may have a different structure to typical extra-tropical cyclones (e.g., Tanaka et al., 2012; Aizawa et al., 2014; Aizawa and Tanaka, 2016; Tao et al., 2017). However, these previous studies only focused on individual case studies, therefore the generality in the development and structure of Arctic cyclones has not yet been determined.

This study aims to describe the typical lifetime, structure, and development of a large sample of past intense Arctic cyclones, using a storm compositing methodology. The composite structure of the 100 most intense summer (JJA) and winter (DJF) Arctic cyclones is compared with that of the 100 most intense winter cyclones occurring over the North Atlantic Ocean between 1979-2020, using data from the ERA-5 reanalysis dataset. Overall, this study shows that Arctic summer cyclones are typically longer lived and have a different development in their composite structure to winter Arctic and North Atlantic Ocean extra-tropical cyclones, and to that described in conceptual models such as the Norwegian Cyclone Model (Bjerknes, 1919, 1922) and the Shapiro Keyser Model (Shapiro and Keyser, 1990).



335 – Intense Arctic summer cyclones have longer lifetimes than winter Arctic and North Atlantic Ocean extra-tropical cyclones.

Cyclones are associated with hazardous weather, including high wind speeds and high ocean waves (Thomson and Rogers, 2014; Liu et al., 2016; Waseda et al., 2018). Arctic cyclones can also enhance the break-up sea ice, which may then become mobile and drift toward shipping lanes, creating an additional hazard to shipping, oil exploration and tourism activities (Simmonds and Keay, 2009; Asplin et al., 2012; Parkinson and Comiso, 2013; Peng et al., 2021). It is found that Arctic
340 summer cyclones are typically much longer lived than winter Arctic and North Atlantic Ocean extra-tropical cyclones. The mean lifetime of the 100 most intense Arctic summer cyclones is found to be more than 3 days longer than that of the 100 most intense winter Arctic and North Atlantic Ocean extra-tropical cyclones. Consequently, Arctic summer cyclones may cause prolonged hazardous weather conditions and prolonged disruption to human activities in the Arctic.

345 – The development shown in the composite structure of intense Arctic summer cyclones is different to that of winter Arctic and North Atlantic Ocean extra-tropical cyclones, and to the description given in conceptual models such as the Norwegian Cyclone Model (Bjerknes, 1919, 1922) and Shapiro-Keyser Model (Shapiro and Keyser, 1990).

The development shown in the composite structure of the 100 most intense Arctic summer cyclones shows that they typically undergo a transition from a baroclinic structure to an axi-symmetric cold core structure throughout the troposphere around the time of maximum intensity (i.e., the time of minimum MSLP). This axi-symmetric cold core structure is consistent with
350 previous studies that have analysed past individual Arctic summer cyclone case studies (Tanaka et al., 2012; Aizawa et al., 2014; Aizawa and Tanaka, 2016; Tao et al., 2017). In comparison, the composite structure of the 100 most intense winter Arctic cyclones is similar to that of the 100 most intense North Atlantic Ocean extra-tropical cyclones, with both of the cyclone composites showing a baroclinic structure with high meridional temperature gradients and signs of occlusion throughout their life-cycle. From the time of maximum intensity, the Arctic summer cyclone composite has a much lower-lying tropopause
355 and a larger positive temperature anomaly in the stratosphere at the centre of the cyclone composite than the winter Arctic and North Atlantic Ocean extra-tropical cyclone composites. The Arctic summer cyclone composite retains this axi-symmetric cold core structure long after the time of maximum intensity.

This composite structural development is found to be different to that of winter North Atlantic Ocean extra-tropical cyclones and winter Arctic cyclones. This is also different to the structural development of extra-tropical cyclones described in the
360 Norwegian Cyclone Model (Bjerknes, 1919, 1922) and Shapiro-Keyser Model (Shapiro and Keyser, 1990). The Arctic summer cyclone composite also shows differences to the Arctic Cyclone Model proposed by Aizawa and Tanaka (2016). This raises questions such as whether this unique structural transition of Arctic summer cyclones is captured in climate model projections and weather forecasting models, and how might the frequency of these Arctic summer cyclones change in response to climate change?

365 It is plausible that the structural transition of Arctic summer cyclones, which don't fully undergo occlusion, may contribute to extending the lifetimes of such cyclones. Arctic summer cyclones may lack the dynamical forcing from the occlusion process that typically helps to force the movement of air that leads to the dissipation of extra-tropical cyclones. The Arctic summer



370 cyclone composite is also found to have a lower tropopause and greater temperature anomaly in the stratosphere at the centre than the winter Arctic and North Atlantic Ocean extra-tropical cyclone composites. This suggests that they may be more strongly influenced by the stratosphere and, in particular, Tropopause Polar Vortices (TPVs) that are common features based on the tropopause in the Arctic (Cavallo and Hakim, 2010). Recent studies have suggested that some Arctic cyclones may have been strongly influenced by TPVs (e.g., Tao et al., 2017; Gray et al., 2021). Understanding what causes this structural transition of Arctic summer cyclones and why they tend to have longer lifetimes than winter Arctic and extra-tropical cyclones is an area for future research.

375 *Data availability.* Data sets for this research are available in these in-text data citation references and the associated repositories. ERA5 reanalysis data (Hersbach et al., 2020). The TRACK algorithm is available on the University of Reading's Git repository (GitLab) at <https://gitlab.act.reading.ac.uk/track/track2021> (Hodges, 2021).

Author contributions. Alexander F. Vessey conducted all of the analysis detailed in this paper and took responsibility to write this paper. Kevin I. Hodges, Len C. Shaffrey and Jonathan J. Day assisted with this analysis and writing.

380 *Competing interests.* The contact author has declared that neither they nor their co-authors have any competing interests.

Acknowledgements. The authors acknowledge the funding and support from the Scenario NERC Doctoral Training Partnership Grant (NE/L002566/1) and co-sponsor, AXA XL, in the development of this research. The authors would also like to acknowledge the European Centre for Medium-Range Weather Forecasts (ECMWF) for the production of ERA-5 reanalysis dataset. The work described in this paper has received funding from the European Union's Horizon 2020 Research and Innovation programme through Grant agreement no. 727862
385 APPLICATE. The content of the article is the sole responsibility of the author(s) and it does not represent the opinion of the European Commission, and the Commission is not responsible for any use that might be made of information contained. Finally, we thank the anonymous reviewers for their constructive comments that helped to improve this manuscript.



References

- Aizawa, T. and Tanaka, H.: Axisymmetric structure of the long lasting summer Arctic cyclones, *Polar Sci.*, 10, 192–198, 2016.
- 390 Aizawa, T., Tanaka, H., and Satoh, M.: Rapid development of Arctic cyclone in June 2008 simulated by the cloud resolving global model NICAM, *Meteorol. Atmos. Phys.*, 126, 105–117, 2014.
- Asplin, M. G., Galley, R., Barber, D. G., and Prinsenberg, S.: Fracture of summer perennial sea ice by ocean swell as a result of Arctic storms, *J. Geophys. Res.: Oceans*, 117, 2012.
- Babin, J., Lasserre, F., and Pic, P.: Arctic shipping and polar seaways, *Encyclopedia of water: science, technology, and society*, 2020.
- 395 Bauer, M. and Del Genio, A. D.: Composite analysis of winter cyclones in a GCM: Influence on climatological humidity, *Journal of climate*, 19, 1652–1672, 2006.
- Bengtsson, L., Hodges, K. I., Esch, M., Keenlyside, N., Kornblueh, L., Luo, J.-J., and Yamagata, T.: How may tropical cyclones change in a warmer climate?, *Tellus*, 59, 539–561, 2007.
- Bengtsson, L., Hodges, K. I., and Keenlyside, N.: Will extra-tropical storms intensify in a warmer climate?, *J. Clim.*, 22, 2276–2301, 2009.
- 400 Bjerknes, J.: On the structure of moving cyclones, *Mon. Weather Rev.*, 47, 95–99, 1919.
- Bjerknes, J.: Life cycle of cyclones and the polar front theory of atmospheric circulation, *Geophys. Publik.*, 3, 1–18, 1922.
- Browning, K.: The dry intrusion perspective of extra-tropical cyclone development, *Meteor. Appl.*, 4, 317–324, 1997.
- Browning, K.: The sting at the end of the tail: Damaging winds associated with extra-tropical cyclones, *Q. J. R. Meteorol. Soc.*, 130, 375–399, 2004.
- 405 Carlson, T. N.: Airflow through mid-latitude cyclones and the comma cloud pattern, *Mon. Weather Rev.*, 108, 1498–1509, 1980.
- Catto, J. L., Shaffrey, L. C., and Hodges, K. I.: Can climate models capture the structure of extra-tropical cyclones?, *J. Clim.*, 23, 1621–1635, 2010.
- Cavallo, S. M. and Hakim, G. J.: Composite structure of tropopause polar cyclones, *Mon. Weather Rev.*, 138, 3840–3857, 2010.
- Clancy, R., Bitz, C. M., Blanchard-Wrigglesworth, E., McGraw, M. C., and Cavallo, S. M.: A cyclone-centered perspective on the drivers of asymmetric patterns in the atmosphere and sea ice during Arctic cyclones, *Journal of Climate*, 35, 73–89, 2022.
- 410 Crawford, A. D. and Serreze, M. C.: Does the summer Arctic frontal zone influence Arctic Ocean cyclone activity?, *J. Clim.*, 29, 4977–4993, 2016.
- Dacre, H.: A review of extra-tropical cyclones: observations and conceptual models over the past 100 years, *Weather*, 75, 4–7, 2020.
- Dacre, H., Hawcroft, M., Stringer, M., and Hodges, K.: An extra-tropical cyclone atlas: A tool for illustrating cyclone structure and evolution characteristics, *Bull. Am. Meteorol. Soc.*, 93, 1497–1502, 2012.
- 415 Gray, S. L., Hodges, K. I., Vautrey, J. L., and Methven, J.: The role of tropopause polar vortices in the intensification of summer Arctic cyclones, *Weather and Climate Dynamics Discussions*, pp. 1–31, 2021.
- Harsem, Ø., Heen, K., Rodrigues, J., and Vassdal, T.: Oil exploration and sea ice projections in the Arctic, *The Polar Record*, 51, 91, 2015.
- Hersbach, H., Bell, B., Berrisford, P., Hirahara, S., Horányi, A., Muñoz-Sabater, J., Nicolas, J., Peubey, C., Radu, R., Schepers, D., et al.: The ERA5 global reanalysis, *Q. J. R. Meteorol. Soc.*, 146, 1999–2049, 2020.
- 420 Hodges, K. I.: A general method for tracking analysis and its application to meteorological data, *Mon. Weather Rev.*, 122, 2573–2586, 1994.
- Hodges, K. I.: Feature tracking on the unit sphere, *Mon. Weather Rev.*, 123, 3458–3465, 1995.
- Hodges, K. I.: Adaptive constraints for feature tracking, *Mon. Weather Rev.*, 127, 1362–1373, 1999.



- Hodges, K. I.: TRACK tracking and analysis system for weather, climate and ocean data, Gitlab [code], pp. Accessed 09 Nov 2020, <https://gitlab.act.reading.ac.uk/track/track2021>, 2021.
- 425
- Leckebusch, G. C., Ulbrich, U., Fröhlich, L., and Pinto, J. G.: Property loss potentials for European midlatitude storms in a changing climate, *Geophys. Res. Lett.*, 34, 2007.
- Li, X., Otsuka, N., and Brigham, L. W.: Spatial and temporal variations of recent shipping along the Northern Sea Route, *Polar Science*, 27, 100569, 2021.
- 430
- Liu, Q., Babanin, A. V., Zieger, S., Young, I. R., and Guan, C.: Wind and wave climate in the Arctic Ocean as observed by altimeters, *J. Clim.*, 29, 7957–7975, 2016.
- Maher, P. T.: Tourism futures in the Arctic, in: *The Interconnected Arctic — UArctic Congress 2016*, pp. 213–220, Springer, Cham, 2017.
- Martínez-Alvarado, O., Baker, L. H., Gray, S. L., Methven, J., and Plant, R. S.: Distinguishing the cold conveyor belt and sting jet airstreams in an intense extra-tropical cyclone, *Mon. Weather Rev.*, 142, 2571–2595, 2014.
- 435
- Melia, N., Haines, K., and Hawkins, E.: Sea ice decline and 21st century trans-Arctic shipping routes, *Geophys. Res. Lett.*, 43, 9720–9728, 2016.
- National Snow & Ice Data Centre: Sea Ice Index Animation Tool, pp. Accessed 11 Nov 2020, https://nsidc.org/data/seaice_index/archives/image_select, 2020.
- Parkinson, C. L. and Comiso, J. C.: On the 2012 record low Arctic sea ice cover: Combined impact of preconditioning and an August storm, *Geophys. Res. Lett.*, 40, 1356–1361, 2013.
- 440
- Peng, L., Zhang, X., Kim, J.-H., Cho, K.-H., Kim, B.-M., Wang, Z., and Tang, H.: Role of intense Arctic storm in accelerating summer sea ice melt: an in situ observational study, *Geophys. Res. Lett.*, 48, e2021GL092714, 2021.
- Pinto, J. G., Karremann, M. K., Born, K., Della-Marta, P. M., and Klawa, M.: Loss potentials associated with European windstorms under future climate conditions, *Climate Research*, 54, 1–20, 2012.
- 445
- Reed, R. J. and Kunkel, B. A.: The Arctic circulation in summer, *J. Meteorol.*, 17, 489–506, 1960.
- Schultz, D. M. and Browning, K. A.: What is a sting jet?, *Weather*, 72, 63–66, 2017.
- Schultz, D. M., Keyser, D., and Bosart, L. F.: The effect of large-scale flow on low-level frontal structure and evolution in mid-latitude cyclones, *Mon. Weather Rev.*, 126, 1767–1791, 1998.
- Serreze, M. C., Lynch, A. H., and Clark, M. P.: The Arctic frontal zone as seen in the NCEP-NCAR reanalysis, *J. Clim.*, 14, 1550–1567, 450 2001.
- Shapiro, M. A. and Keyser, D.: Fronts, jet streams and the tropopause, in: *Extratropical Cyclones: The Eric Palmen Memorial Volume*, pp. 167–191, Springer, 1990.
- Simmonds, I. and Keay, K.: Extraordinary September Arctic sea ice reductions and their relationships with storm behavior over 1979–2008, *Geophys. Res. Lett.*, 36, 2009.
- 455
- Simmonds, I. and Rudeva, I.: The great Arctic cyclone of August 2012, *Geophys. Res. Lett.*, 39, 2012.
- Simmonds, I., Burke, C., and Keay, K.: Arctic climate change as manifest in cyclone behavior, *J. Clim.*, 21, 5777–5796, 2008.
- Stroeve, J., Holland, M. M., Meier, W., Scambos, T., and Serreze, M.: Arctic sea ice decline: Faster than forecast, *Geophys. Res. Lett.*, 34, 2007.
- Stroeve, J. C., Kattsov, V., Barrett, A., Serreze, M., Pavlova, T., Holland, M., and Meier, W. N.: Trends in Arctic sea ice extent from CMIP5, 460 CMIP3 and observations, *Geophys. Res. Lett.*, 39, 2012.



- Tanaka, H. L., Yamagami, A., and Takahashi, S.: The structure and behavior of the Arctic cyclone in summer analyzed by the JRA-25/JCDAS data, *Polar Sci.*, 6, 55–69, 2012.
- Tao, W., Zhang, J., and Zhang, X.: The role of stratosphere vortex downward intrusion in a long-lasting late-summer Arctic storm, *Q. J. R. Meteorol. Soc.*, 143, 1953–1966, 2017.
- 465 Thomson, J. and Rogers, W. E.: Swell and sea in the emerging Arctic Ocean, *Geophys. Res. Lett.*, 41, 3136–3140, 2014.
- Vessey, A. F., Hodges, K. I., Shaffrey, L. C., and Day, J. J.: An inter-comparison of Arctic synoptic scale storms between four global reanalysis datasets, *Clim. Dyn.*, 54, 2777–2795, 2020.
- Wang, C.-C. and Rogers, J. C.: A composite study of explosive cyclogenesis in different sectors of the North Atlantic. Part I: Cyclone structure and evolution, *Monthly Weather Review*, 129, 1481–1499, 2001.
- 470 Waseda, T., Webb, A., Sato, K., Inoue, J., Kohout, A., Penrose, B., and Penrose, S.: Correlated increase of high ocean waves and winds in the ice-free waters of the Arctic Ocean, *Sci. Rep.*, 8, 1–9, 2018.